ISSN 2070-2051, Protection of Metals and Physical Chemistry of Surfaces, 2019, Vol. 55, No. 2, pp. 302–309. © Pleiades Publishing, Ltd., 2019.

NANOSCALE AND NANOSTRUCTURED MATERIALS AND COATINGS

Electrophoretic Deposition of Nanobiocomposites for Orthopedic Applications: Influence of Contained Water in Suspension

A. Molaei[a] and M. A. Yousefpour[b, *]

[a] *Department of Materials Engineering, Tehran Science and Research Branch, Islamic Azad University, Tehran, 14778-93855 Iran*

[b] *Faculty of Materials and Metallurgical Engineering, Semnan University, Semnan, 35131-19111 Iran*

**e-mail: myousefpor@semnan.ac.ir*

Received November 22, 2017; revised September 8, 2018; accepted October 10, 2018

Abstract—Chitosan (CS) nanocomposite coatings containing bioglass 45s5 (BG), hydroxyapatite (HA), and halloysite nanotube (HNT) were developed on Titanium (Ti) by electrophoretic deposition (EPD) from ethanol-water suspensions. The optimal water ratio in the ethanolic suspension was studied in order to avoid the bubble formation during the EPD process and to ensure homogeneous coatings. The smooth and non-agglomerated coating was fabricated in the ethanol-based suspension containing 30% water. Coating composition was analyzed by Energy dispersive X-ray (EDX), Fourier transform infrared spectroscopy (FTIR), and X-ray diffraction (XRD) analyses. Scanning electron microscopy (SEM) was employed to study the surface morphology of the coatings. The electrochemical behavior of the coatings, evaluated by polarization curves and Nyquist plots in the corrected simulated body fluid (C-SBF) at 37°C, was studied in order to assess the corrosion resistance of the Ti substrate.

Keywords: electrophoretic, electrophoresis, electrolysis, water, coating

DOI: 10.1134/S2070205119020217

1. INTRODUCTION

A wide variety of materials have been utilized for fabricating biocomposites [1, 2]. These have been categorized in specific groups: ceramics, like hydroxyapatite (HA) and halloysite nanotube (HNT), glasses, such as bioglass 45s5 (BG), polymers, like chitosan (CS), and metallic biomaterials, like Titanium (Ti) [3]. Among these materials, metallic biomaterials have found broad applications in orthopedics and dentistry [4]. Metallic biomaterials have high susceptibility to corrosion and to overcome this shortcoming, the surface modification is performed before their usages in the body [5].

There are a lot of methods for the fabrication of biocomposite coatings on the surface of metallic biomaterials [3–6]. The growing interest toward the application of electrophoretic deposition (EPD) in the CS-based coating is ascribed to its simplicity, ability to produce smooth coating, low processing temperature, low cost, and high production rate [7, 8]. In EPD, charged particles, dispersed or suspended in a liquid medium, attract and deposit onto a conductive substrate of opposite charge on the application of a DC electric field. The effective parameters on EPD have been categorized into two groups: (i) those related to the suspension and (ii) those related to the process [6]. A number of factors relating to the composition of suspension including the concentration of contained solvents, particles, additives, and so on [6, 7]. Providing an optimum suspension results in an non-agglomerated and homogeneous coating. Several solvents have been utilized on the base of methanol, ethanol, acetic acid, n-propanol, and isopropylalcohol. Each of them has specific properties and applications [7–10].

One favorite solvent embedded in the suspension for depositing the CS-based coating is water [6, 11]. Adding water in the suspension is useful for dissolving CS polymer and depositing CS-based composites on cathodes. The utilization of water implies advantages such as higher temperature-control during the process or a faster kinetics, in addition to important health, environmental, and cost benefits. However, the water-based suspensions causes a number of problems in the electrophoretic forming. The main problems relate to the electrophoresis of water on electrodes when the current is passed through, which extremely affects the efficiency of the process and the uniformity of deposition [6]. A few scientists have investigated to control the chemistry processes of the water-contained suspensions. Mehdipour [12] evaluated the water amount for fabricating a uniform CS-BG coating on the surface of stainless steel. The study of kinetics of water-embedded suspensions for depositing CS polymer was performed by Simchi [13]. Furthermore, Boccaccini

[14] presented experimental results on the electrophoretic deposition of CS/BG composite coatings in suspensions contained water based on the Taguchi design of experiments (DOE) approach.

In order to move forward to investigate contained water in the electrophoretic suspension, more studies is necessary. The aim of this research is to evaluate the effects of contained water and to fabricate optimized CS-based nanocomposite coating on the Ti surface. The colloidal stability of the suspension containing different water percentages and constituent components were also surveyed. The coating morphology and composition were characterized used SEM, EDX, XRD, and FTIR techniques. Finally, the electrochemical behavior was analyzed by polarization curves and EIS Nyquist spectra to assess the effects of contained water on the corrosion resistance of the Ti substrate.

2. EXPERIMENTAL DETAILS

2.1. Materials

Chitosan with medium molar mass, acetic acid, ethanol, silicon dioxide (SiO_2), sodium carbonate anhydrous ($NaCO_3$), calcium carbonate ($CaCO_3$), phosphorus pentoxide (P_2O_5), calcium nitrate tetrahydrate ($Ca(NO_3)_2 \cdot 4H_2O$), and halloysite nanotube ($Al_2Si_2O_5(OH)_4 \cdot 2H_2O$) were purchased from Sigma-Aldrich. BG and HA powders were prepared by melting and sol-gel techniques, respectively [15, 16]. The particle size of BG is less than 37 μm and HA is less than 150 nm (as the median).

2.2. Electrophoretic Deposition

The mixed ethanol-water solvent was chosen for the electrophoretically deposition of the CS-based nanocomposite coating. Dilute CS solution was prepared by dissolving 0.5 g/L CS in 1% acetic acid solution and stirring for 24 h at room temperature. Materials with the concentration of 0.7 g/L BG, 0.7 g/L HA, and 0.6 g/L HNT powders were added to the ethanol-water solvent. Prior to EPD, the dispersion was performed by stirring for 120 min and then sonicating for 21 min to achieve an homogeneous distribution. The deposition was performed at the voltage of 30 V and the deposition duration of 5 min in the suspensions containing different ranges of water from 17 to 60%.

The EPD cell setup consists of a Ti plate of $1 \times 20 \times 35$ mm^3 and a 316L stainless steel plate of $1 \times 21 \times 37$ mm^3 as a cathode and an anode, respectively. A constant distance of 15 mm was designed between electrodes. The surface of electrodes were polished by SiC abrasive papers and then rinsed with deionized water and ethanol. Ti was degreased with acetone in an ultrasonic bath and etched in a solution containing nitric acid (HNO_3) and hydrofluoric acid (HF) (1 : 1 ratio in volume) for 10 s following with rinsing in ethanol and water and then drying.

2.3. Characterization

In order to characterize the nanocomposite coatings, XRD (3003 PTS, Seifert), FTIR (Thermo Nicolet NEXUS 870), SEM (JXA-840, JEOL), EDX (Oxford Instruments) were used.

The electrochemical behavior of the coatings was also studied in order to test the effect of contained water in the suspension on their possible protective properties. Potentiodynamic polarization curves were carried out used polarization tests and electrochemical impedance spectroscopies (EG and G model 273 A) in the corrected simulated body fluid (C-SBF) at 37°C. C-SBF solution was prepared according to the procedure described by Kokubo and Takadama [17]. The counter and the reference electrodes were platinum plate and standard calomel electrode (SEC), respectively. The impedance spectra were acquired in the frequency range of 0.1 mHz to 0.1 MHz with a 5 mV amplitude.

3. RESULTS AND DISCUSSION

3.1. Stability of CS-based Suspension

The charging process of particles is very slow in the organic solvents with weak acid-based properties and the addition of a suitable value of acetic acid can accelerate the charging process of constituted particles. From another aspect, the excessive acetic acid can accelerate the generation process of hydrogen on the cathode, which would interfere with the deposition process. It can be concluded that the quantity of acetic acid in the electrolyte has a significant effect on the EPD. In the past research, we studied the added amount of acetic acid contained in deionized water and found out that 1% V acetic acide yield excellent CS distribution and subsequently optimum satisfactory deposition coating [18, 19].

It is approved that the suspensions of ceramic particles were unstable and showed fast sedimentation. These suspensions are indesirable for EPD. For improving the stability of suspension, CS polymer as charging and dispersing agent is used. The outstanding mechanism is that, in the CS-based solution, the salt form of CS dissociates to polycations with a charge that depends on its molecular weight and deacetylation degree (DA) as well as negatively charged counter ions. CS alters the surface property of contained ceramic particles in the suspension and augments their Zeta potentials and mobilities [18, 19].

In our past research about the fabrication of CS/HNT, we found out that CS does not adequately dissolve in the pure ethanol and also dissolving of CS in the pure water is probable, though significant amounts of hydrogen gases form on the cathode's surface during EPD, which eventually leads to the fabrication of a porous structure. Also, it is resulted that increasing of ethanol in the aqueous solvent reduces porosity by decreasing current density. Thus, it is nec-

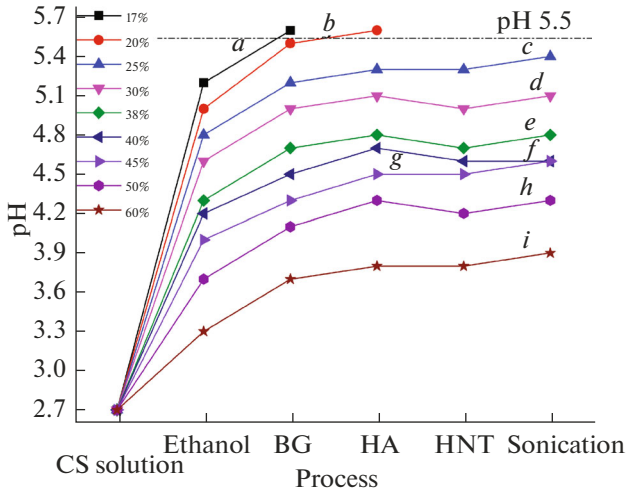

Fig. 1. The effect of added components and taken sonication process on pH in different water% of suspensions: (*a*) 17, (*b*) 20, (*c*) 25, (*d*) 30, (*e*) 38, (*f*) 40, (*g*) 45, (*h*) 50, and (*i*) 60.

essary to achieve an optimum ethanol-water ratio to fabricate a uniform coating while maintain a reasonable deposition rate [18–20].

pH is measured before and after the addition of 0.7 g/L BG, 0.7 g/L HA, and 0.6 g/L HNT powders as well as 20 min sonication in the solutions containing various water percentages and results are presented in Fig. 1.

As it is shown in Fig. 1, after each process, pH increases more in a higher decreasing slop. The reasons of these behaviors present as follows:

The result of Fig. 1 indicates, pH reduces with increasing the water volume or decreasing the ethanol volume. It demonstrates that by adding more water, higher number of hydrogen gases releases in the solvent by dissociating water according to the following reaction.

$$H_2O \rightarrow 2H^+ + OH^-. \quad (1)$$

As it is shown in Fig. 1, by the addition of 0.7 g/L BG and 0.7 g/L HA powders in the aqueous solvent, due to releasing Ca^{2+}, Na^+, and PO_4^{3-} ions as well as adsorbing H^+ ions on the particles, pH increases.

Suspensions containing 0.7 g/L BG and 0.7 g/L HA particles in the solvents with the water ratios of 17 and 20% were unstable and the particles precipitate after about one minute stirring. In these ratios, pH reaches an amount of 5.5, precipitating CS and ceramic particles [18–20].

By introducing HNT particles into the suspension, pH decreases. As in Fig. 2 is shown, due to presenting positive-charged Al_2O_3 on the surface of HNTs and subsequently adsorbing OH^- by the electrostatic forces, pH of the suspension decreases.

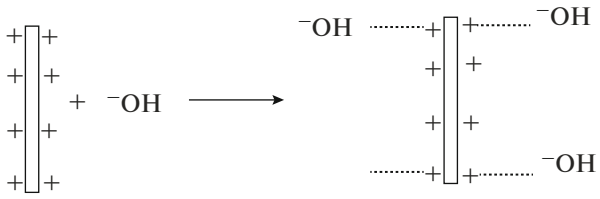

Fig. 2. The electrostatic reaction between HNT nanoparticles and OH^-.

The charging process of ceramic particles in the CS-based suspension needs a certain time of aging to obtain a stable suspension solution [21]. If the suspension solution is not aged, the charged values of particles are a few or zero, therefore, it is difficult to provide the nanocomposite coating no matter how long was the EPD process. After sonicating, by rising temperature resulting in augmenting the number of OH^-, achieving from the water electrolysis, pH amount increases.

During initial time of EPD process, due to releasing of hydrogen gases on the cathode surface, the suspension containing of the ethanol-25% water solvent loses its stability. Also, it is illustrated that because of the electrophoresis of water, the suspensions containing more than 50% water would fabricate ununiform and porous depositions [6, 18–20]. Thus, to investigate the proper contained water among the remained suspensions, contained 30, 38, 40, and 45% water, more analysis is required.

The conductivity of suspension affects its stability and efficiency. As it is exhibited in Fig. 3, increasing of the water percentage and subsequently dissolving of more H^+ and OH^- in the suspension lead to a higher amount of conductivity. Furthermore, adding of components and then decreasing of pH relating to the suspension provides an increase in the conductivity highly related to the ionic strength of the suspension.

As can be observed in Fig. 4, suspensions containing 38 and 45% water fabricate the maximum and minimum weight of coatings, respectively. Furthermore, by rising of water contented in the suspension, the thickness of deposition increases.

High ion concentrations in the suspension cause an increase in the rate of agglomeration and the number of free ions. This large number of free ions may then acts as principal current carriers, reducing the speed of the particles and consequently the deposition rate [22]. Low ion concentration results in decreasing the deposition rate and forming a weak deposition. Ferrari and Moreno [23] found the existence of a narrow band of conductivity range in which the deposition is formed. Conductivity out of this region is not suitable for EPD, limiting the forming possibilities. As it is exhibited in Figs. 3 and 4, rising the water ratio from 38 to 45% increases the conductivity from 132 to

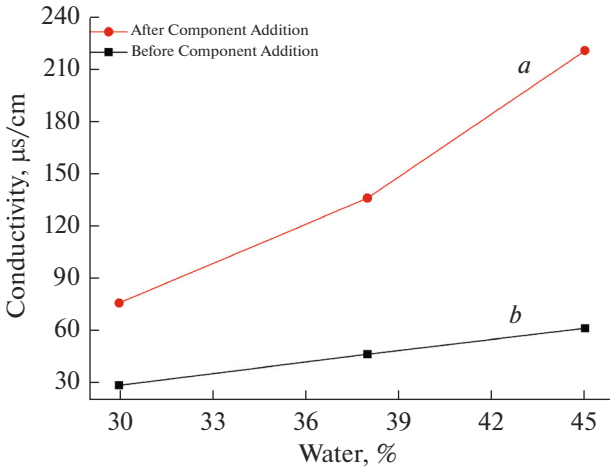

Fig. 3. The dependance of conductivity on the water percentage (a) after and (b) before adding components in the suspension.

224 μs/Cm and reduces the deposition rate from 13.4 to 11.8 μg/cm^2. Thus, in order to achieve a suitable relation between the conductivity and deposition rate to fabricate a uniform and closed-compacted coating, suspensions containing 30 to 38% water have suitable conductivities in the range of 76–132 μs/cm.

3.2. Characterization of the Coating

3.2.1. SEM and EDX study. Fig. 5 shows deposited samples with different water contents in the suspension.

Increasing water content in the suspension changes the morphology of coatings. Figs. 5a, 5b depict smooth and dense coatings with low cracks and agglomerations in high and low magnifications, respectively. By increasing of water content in the suspension from 30 to 38%, more cracks and porosity as well as agglomerations observe on the nanocomposite coating (Figs. 5c, 5d, 5e). As it is observable in Figs. 5f, 5g, flaked composite coatings with the large number of cracks and porosity are fabricated in the suspension containing 45% water. Also, Fig. 5h illustrates HNT agglomerations fabricated in the ethanol-45% water suspension.

By increasing water content, more hydrogen gas releases on the surface of cathode and therefore more porosity and cracks appear. Moreover, with the addition of water, a high conductivity and number of free ions in the suspension result in increasing the ionic resistance. This behavior has a significant impact on forming larger agglomerations and wider cracks and porosity.

Fig. 4 has a good agreement with the result that is demonstrated in Fig. 2.

The CS-based nanocomposite coatings fabricated in the ethanol-45% water suspension have unsuitable

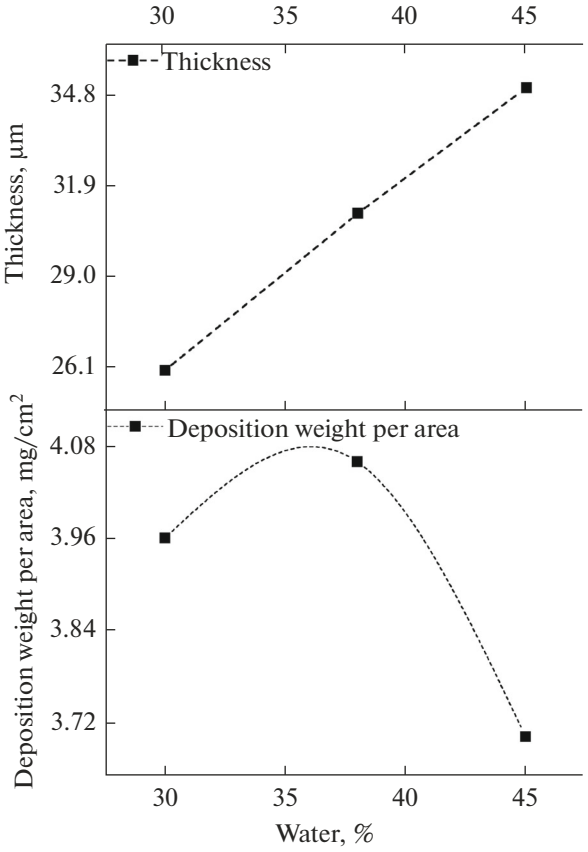

Fig. 4. The coating weight per unite of surface area and thickness as a function of embedded water percentage in the suspension.

adhesion to the substrate, which results from a high amount of cracks and porosity. The CS-based coating adhesion is evaluated according to the ASTM D3359 standard characterized that the adhesion strength attributing to the 0B classification.

The effective parameters on the formation of cracks and porosity of nanocomposite coating can be listed as follows:

(I) The revolted gases forming bubbles in the size of about 5 μm, because of the low voltage threshold for the water electrolysis [24].

(II) The CS shrinkage that obtains after the drying and dehydration processes [21].

(III) Significant difference in the dimension and shape of particles [19].

It is approved that increasing and decreasing of porosity in composites have advantageous and disadvantageous effects on the medical and surface engineering. In spite of the fact that an increase in porosity causes an improvement in the contacting area for the cell attachment and spreading, weakening of coating's the adhesion strength would be achieved [25].

The EDS spectrum of the CS-based nanocomposite coating illustrates the presence of Ca and P relating

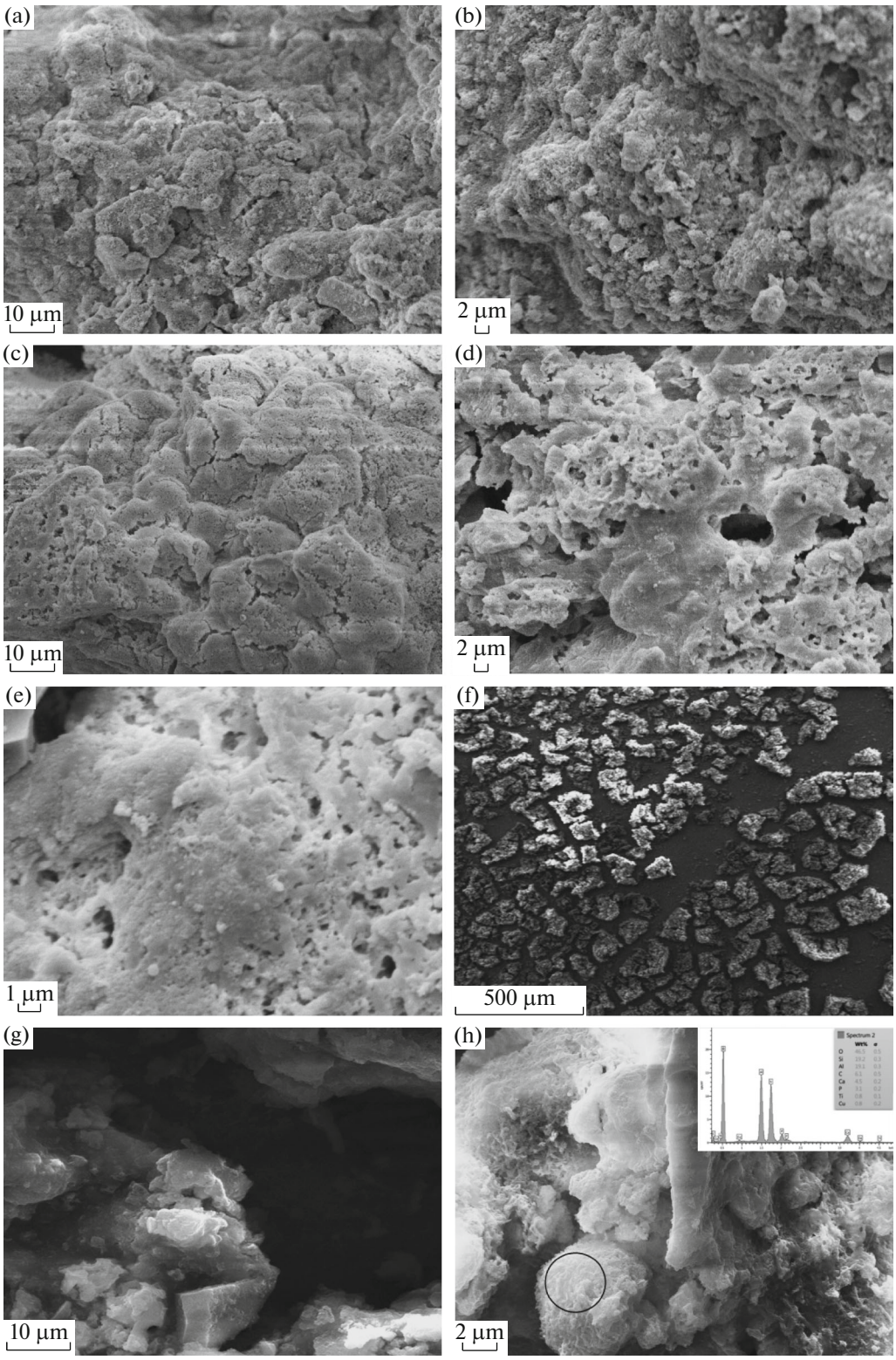

Fig. 5. SEM of the CS-based coatings fabricated from the suspension containing (a, b) 30%, (c, d, e) 38%, (f, g) 45% water, and (h) EDX of the CS-based coating fabricated in the ethanol-30% water suspension.

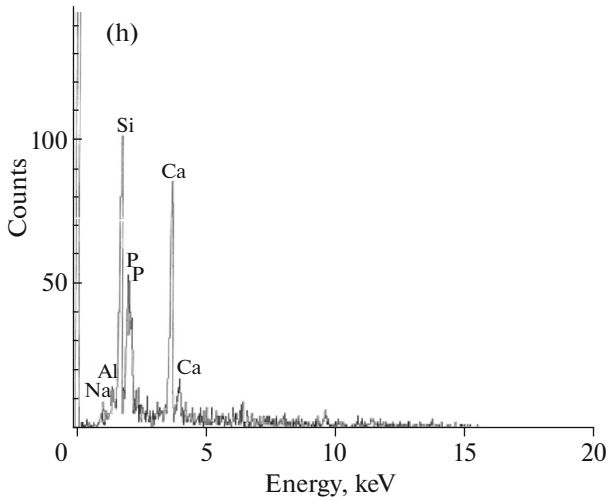

Fig. 5. (Contd.)

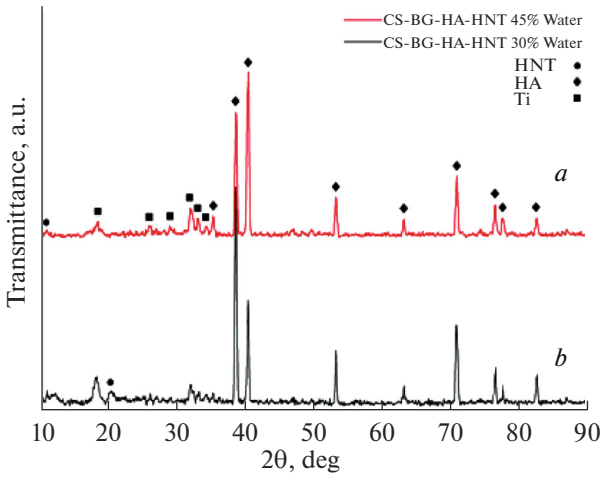

Fig. 6. XRD spectrum of the CS-based nanocomposite coatings fabricated in the suspension containing (*a*) 45 and (*b*) 30% water.

to BG and HA and Al relating to Hal nanotubes in the composition (Fig. 4h).

Therefore, it is verifiable that EPD at the suspension containing a low water content (30%) achieves a great morphology.

3.2.2. XRD and FTIR analyses. Fig. 6 compares XRD patterns of the CS-based composite coatings fabricated in the suspensions with different water contents. The diffracted peaks are characterized relating to HA and HNT nanoparticles as well as Ti substrate, but no peaks are indicated relating to CS and BG. Chitosan is deposited in the semi-crystalline form. As shown in Fig. 6, HA and HNT peaks have lower intensity in curve a compared with curve b. It is indicated that owing to more conductivity, in the suspension containing a high amount of water, particles deposit in a lower rate on the Ti substrate.

FTIR analyses of BG powder and CS-based composite deposited in the ethanol-30% water suspension are represented in Fig. 7. By comparing Figs. 7a, 7b, the deposition of biogass microparticles in the composite coating is observable. The peak around 466 cm^{-1} is due to the stretching modes of Si–O–Si and P–O bonds. 568 cm^{-1} is relating to the bending bonds of Si–O–Si, Al–O–Si, and P–O [26]. C–O has stretching mode at 760 and 870 cm^{-1}. The wavenumber of 915 cm^{-1} is pertaining to the stretching bonds of Si–O–Si and C–O. The bonds near 1020–1070 cm^{-1} are belonging to CO of the ring COH, COC, and CH_2OH and also in-plane Si–O stretching of HNTs, as well as P–O bond [20]. The bonds at 1420 and 2927 cm^{-1} show the symmetric stretching bond of C–H in CH_2 and CH_3. Peaks at 1484, 2356, and 3427 cm^{-1} are relating to hydroxyl groups and CO_2 adsorbed from the atmosphere. The intercalated water of HNT and adsorbed water are relating to 3448 cm^{-1}. The presence of the hydroxyl group is relating to HNT particles is assigned

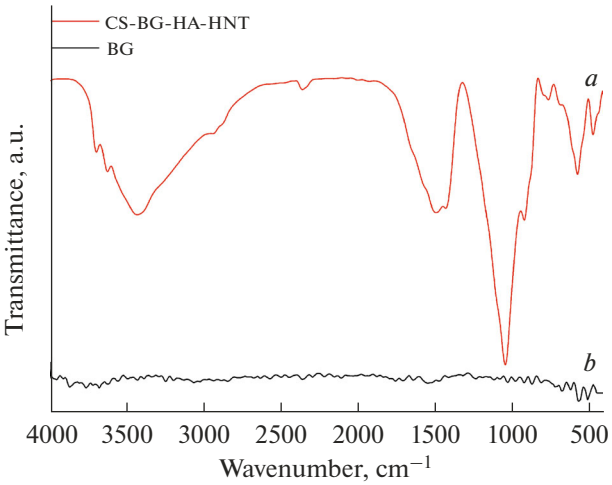

Fig. 7. FTIR spectra of (*a*) the CS-based nanocomposite coating fabricated in the suspension contains 30% water and (*b*) BG particle.

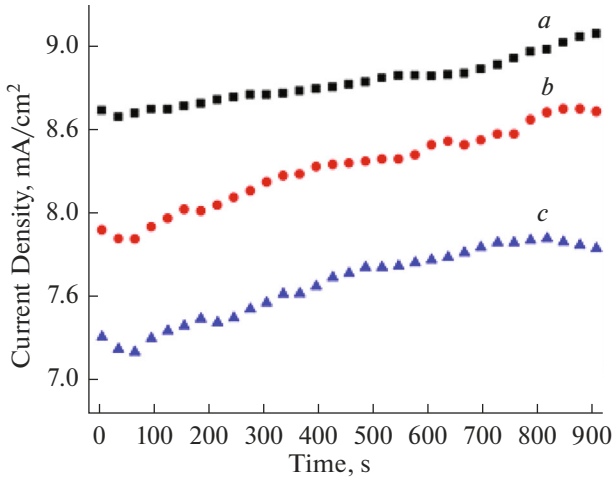

Fig. 8. *i–t* curve of the suspension at different water percentages of (*a*) 30, (*b*) 38, and (*c*) 45.

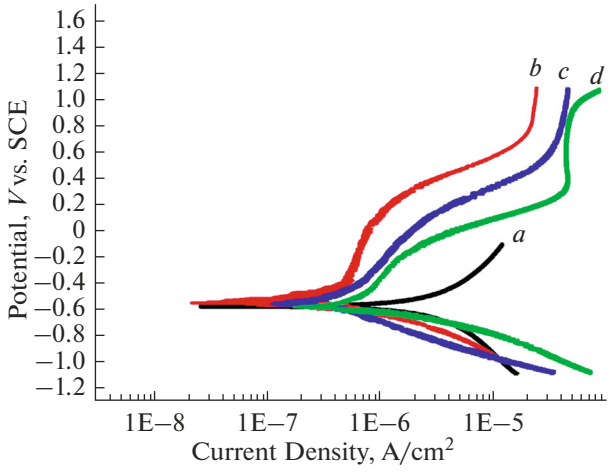

Fig. 9. Potentiodynamic polarization curves for (*a*) bare and CS-based composite coated Ti fabricated in the suspension containing (*b*) 30, (*c*) 38, and (*d*) 45% water in C-SBF at 37°C.

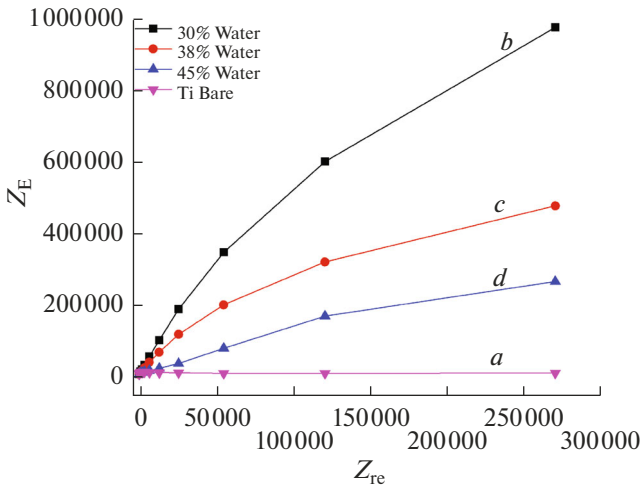

Fig. 10. Impedance spectra for (*a*) uncoated and CS-based composite coated Ti fabricated in the suspension containing (*b*) 30, (*c*) 38, and (*d*) 45% water in C-SBF at 37°C.

at 3628 and 3688 cm^{-1}, as each -OH is linked to two Al atoms and form Al_2OH-stretching mode and also the stretching bond of Si–O–Si as well as P–O bond [19].

3.3. Chronoamprometric Analysis

Fig. 8 exhibits *i–t* curves for the CS-based coating obtained at different water percentages in the suspension. The ascending trend is visible in the current density with time. Descending trend observes for initial time attributing to the shielding effect of the deposited layer (barrier layer). After this drop, the ascribing behavior is pertaining to transporting ions from holes of HNTs via the capillary behavior and diffusing ions from gellish CS. The maximum and minimum current densities are attributing to the water contents of 45 and 30%, respectively.

Different mechanisms have been introduced for the EPD of the CS-based nanocomposite coatings [18–20]. Protonated chitosan dissolves in the ethanol-water mixture at low pH. Under this condition, the amine groups of chitosan protonate, according to following reaction:

$$\text{Chit-NH}_2 + \text{H}_3\text{O}^+ \rightarrow \text{Chit-NH}_3^+ + \text{H}_2\text{O}. \quad (2)$$

Protonated amino groups of CS (NH_3^+) chelate and then surround particles. At the initial deposition times, self-assembled HA and HNT nanoparticles chelate by the cationic macromolecular chains and significantly join to BG microparticles. The reason for this behavior is relating to the dimension difference of constituent particles. Ceramic particles smoothly distribute in the polymeric matrix. By raising the barrier layer, the CS-coated particulates with HA and HNT mainly form in the suspension and then they move towards the surface of the cathode under the influence of applied voltage.

During the EPD process, the electrolysis of water occurs that increases the local pH at the cathode (according to equations (3) and (4)).

$$2\text{H}_2\text{O} + 2\text{e}^- \rightarrow \text{H}_2 + 2\text{OH}^-, \quad (3)$$

$$\text{O}_2 + 2\text{H}_2\text{O} + 4\text{e}^- \rightarrow 4\text{OH}^-. \quad (4)$$

Consequently, according to reaction 5, the protonated amine-groups of chitosan and ceramic particles lose their charges in the high pH region to form an insoluble deposition as described in our another study [19] that the electrophoretic mobility of particles depends on the pH and the conductivity of the suspension.

$$\text{Chit-NH}_3^+ + \text{OH}^- \rightarrow \text{Chit-NH}_2 + \text{H}_2\text{O}. \quad (5)$$

3.5. Corrosion Resistance Study

Fig. 9 exhibits the polarization curves of the bare and coated substrates prepared from the suspensions with different water percentages in the C-SBF solution. Values of E and I for the corrosion points extracted from these curves are listed in Table 1. The results show a lower corrosion current for all coated Ti

Table 1. *I* and *E* for for the corrosion points of bare and coated Ti obtained at different water amounts of the suspension

	Ti pure	30% Water	38% Water	45% Water
E_{corr}, V	–0.587	–0.51	–0.518	–0.559
I_{corr}, μA/cm^2	91.2	0.578	0.591	0.834

in comparison with the bare Ti, being proof of the corrosion protective properties of these coatings.

Fig. 10 depicts the EIS Nyquest spectra of the CS based composite coated Ti. Great amounts of impedance in the coated samples indicate the most likely a passive behavior in the C-SBF solution.

According to the polarization and impedance test results, it is obvious that the corrosion potential reduces and corrosion current increases by adding of the water amount from 30 to 45% in the suspension due to the barrier effect of coating. In the polarization test in contrast with the impedance test, there is no visible difference between the corrosion resistances of samples deposited in the suspensions containing 30 and 38% water. The reason for this mismatch is more dissolution of embedded CS polymer during the polarization than impedance test [19]. The additional water percentage from 38 to 45, significantly increases the current density from 0.591 $\mu A/cm^2$ to a value of 0.834 $\mu A/cm^2$. By forming a high amount of cracks and porosity on the surface of coating fabricated from the suspension containing 45% water, openings achieve for transporting ions and corroding the Ti substrate.

4. RESULTS

CS-based nanocomposite coatings in the suspensions containing different water percentages were prepared on the Ti substrate by the EPD technique. It was found by the results of pH and conductivity measurements, ethanolic suspensions containing water range of 30–38% were introduced as the stable and optimized suspensions. Furthermore, SEM, EDX, XRD, FTIR analyses as well as corrosion resistance tests illustrated that a uniform and non-agglomerated nanocomposite coating is fabricated from the ethanol-30% water suspension. The deposition mechanism of composite coating containing CS polymer with BG, HA, and HNT ceramics was investigated. Corrosion resistance improvement could be obtained by the formation of nanocomposite coating on the Ti substrate.

REFERENCES

1. Sun, F., Zhou, H., and Lee, J., *Acta Biomater.,* 2011, vol. 7, p. 3813.
2. Lian, Z., Guan, H., Ivanovski, S., Loo, Y.C., Johnson, N.W., and Zhang, H., *Int. J. Oral Maxillofac. Surg.,* 2010, vol. 39, p. 690.
3. Caridade, S.G., Merino, E.G., Alves, N.M., and Mano, J.F., *Mater. Sci. Eng., C,* 2013, vol. 33, p. 4480.
4. Zhitomirsky, I. and Hashambhoy, A., *J. Mater. Process. Technol.,* 2007, vol. 191, p. 68.
5. Pinheiro, A.C., Bourbon, A.I., Quintas, M.A.C., Coimbra, M.A., and Vicente, A.A., *Innovative Food Sci. Emerging Technol.,* 2012, vol. 16, p. 227.
6. Laxmidhar, B., and Meilin, L., *Prog. Mater. Sci.,* 2007, vol. 52, p. 1.
7. Li, Y., Wu, K., and Zhitomirsky, I., *Colloids Surf., A,* 2010, vol. 356, p. 63.
8. Batmanghelich, F. and Ghorbani, M., *Ceram. Int.,* 2013, vol. 5, p. 5392.
9. Simchi, A., Tamjid, E., Pishbin, F., and Boccaccini, A.R., *Nanomedicine,* 2011, vol. 7, p. 22.
10. Liang, D., Lu, Zh., Yang, H., Gao, J., and Chen, R., *ACS Appl. Mater. Interfaces,* 2016, vol. 8, p. 3958.
11. Lu, Z., Gao, J., He, Q., Wu, J., Liang, D., Yang, H., and Chen, R., *Carbohydr. Polym.,* 2017, vol. 156, p. 460.
12. Mehdipour, M. and Afshar, A., *Ceram. Int.,* 2012, vol. 38, p. 471.
13. Simchi, A., Pishbin, F., and Boccaccini, A.B., *Mater. Lett.,* 2009, vol. 63, p. 2253.
14. Pishbin, F., Simchi, A., Ryan, M.P., and Boccaccini, A.R., *Surf. Coat. Technol.,* 2011, vol. 205, p. 5260.
15. Ramezanzadeh, B., Arman, S., Mehdipour, M., and Markhali, B., *Appl. Surf. Sci.,* 2014, vol. 289, p. 129.
16. Naghib, S.M., Ansari, M., Pedram, A., Moztarzadeh, F., Feizpour, A., and Mozafari, M., *Int. J. Electrochem. Sci.,* 2012, vol. 7, p. 2890.
17. Kokubo, T. and Takadama, H., *Biomaterials,* 2006, vol. 27, p. 2907.
18. Simchi, A., Pishbin, F., and Boccaccini, A.B., *Mater. Lett.,* 2009, vol. 63, p. 2253.
19. Molaei, A., Amadeh, A., Yari, M., and Afshar, M.R., *Mater. Sci. Eng.*, C, 2016, vol. 59, p. 740.
20. Molaei, A., Yari, M., and Afshar, M.R., *Ceram. Int.,* 2015, vol. 41, p. 14537.
21. Molaei, A., Yari, M., and Afshar, M.R., *Appl. Clay Sci.,* 2016, vol. 135, p. 75.
22. Molaei, A., Yousefpour, M.A., *Int. J. Polym. Mater.*, 2018, DOI:10.1080/00914037.2018.1493683.
23. Deen, I., and Zhitomirsky, I., *J. Alloys Compd.*, 2014, vol. 586, p. 531.
24. Vergaro, V., Abdullayev, E., Lvov, Y.M., Zeitoun, A., Cingolani, R., Rinaldi, R., and Leporatti, S., *Biomacromolecules,* 2010, vol. 11, p. 820.
25. Zhitomirsky, D., Roether, J.A., Boccaccini, A.R., and Zhitomirsky, I., *J. Mater. Process. Technol.,* 2009, vol. 209, p. 1853.
26. Deen, I., Pang, X., and Zhitomirsky, I., *Colloids Surf., A,* 2012, vol. 410, p. 38.